Available online at www.sciencedirect.com

ScienceDirect

International Journal of Thermal Sciences 47 (2008) 1184–1194

International Journal of Thermal Sciences

www.elsevier.com/locate/ijts

Effect of temperature dependent properties on MHD convection of water near its density maximum in a square cavity

S. Sivasankaran *, C.J. Ho

Department of Mechanical Engineering, National Cheng Kung University, Tainan–70101, Taiwan

Received 15 June 2007; received in revised form 3 October 2007; accepted 4 October 2007

Available online 8 November 2007

Abstract

Natural convection of water near its density maximum in the presence of magnetic field in a cavity with temperature dependent properties is studied numerically. The viscosity and thermal conductivity of the water is varied with reference temperature and calculated by cubic polynomial. The finite volume method is used to solve the governing equations. The results are presented graphically in the form of streamlines, isotherms and velocity vectors and are discussed for various combinations of reference temperature parameter, Rayleigh number, density inversion parameter and Hartmann number. It is observed that flow and temperature field are affected significantly by changing the reference temperature parameter for temperature dependent thermal conductivity and both temperature dependent viscosity and thermal conductivity cases. There is no significant effect on fluid flow and temperature distributions for temperature dependent viscosity case when changing the values of reference temperature parameter. The average heat transfer rate considering temperature-dependent viscosity are higher than considering temperature-dependent thermal conductivity and both temperature-dependent viscosity and thermal conductivity. The average Nusselt number decreases with an increase of Hartmann number. It is observed that the density inversion of water leaves strong effects on fluid flow and heat transfer due to the formation of bi-cellular structure. The heat transfer rate behaves non-linearly with density inversion parameter. The direction of external magnetic field also affect the fluid flow and heat transfer.

Keywords: Convection; MHD; Density maximum; Temperature dependent properties

1. Introduction

Convection in a cavity with differentially heated side walls and insulated horizontal surfaces has been studied due to wide range of applications in science, engineering and technology. Natural convection of water around its density maximum is complicated. Some reports on this can be found in literature [1–5]. The process of manufacturing materials in industrial problems involve an electrically conducting fluid subjected to a magnetic field [6–9]. The fluid properties like viscosity and thermal conductivity are varying with temperature in nature. The varying fluid properties are affected the fluid flow and heat transfer within the enclosure [10–12]. Therefore, the consideration of influence of temperature dependent fluid properties in enclosure in the presence of magnetic field is necessary with large temperature differences. In most of the studies presented in literature on natural convection in differentially heated cavity has not been considered the above said effects together. The present work aims to study the effects of temperature dependent fluid properties on natural convection of water in the presence of magnetic filed.

Natural convection of water near its density maximum in rectangular enclosure is investigated by Tong [13]. Ishikawa et al. [14] studied numerically the natural convection with density inversion of water in a cavity. They made a correlation between average Nusselt number and the parameters involved in the study. Natural convection in a square cavity with variable viscosity fluid is investigated by Madhi and Wedgworth [15]. The effects of variable fluid properties on natural convection in a square cavity for different temperature difference ratios is stud-

* Corresponding author.
E-mail addresses: ssiva@mail.ncku.edu.tw (S. Sivasankaran), cjho@mail.ncku.edu.tw (C.J. Ho).

1290-0729/$ – see front matter
doi:10.1016/j.ijthermalsci.2007.10.001

Nomenclature

$\mathbf{B}$	magnetic field	α	thermal diffusivity
c_p	specific heat . . . . . J/kg K	β	volumetric coefficient of thermal expansion
$\mathbf{F}$	electromagnetic force	ϵ	reference temperature parameter
$\mathbf{g}$	acceleration due to gravity . . . . . m/s^2	ϕ	direction of the external magnetic field
H	height of the enclosure . . . . . m	μ	viscosity . . . . . m^2/s
Ha	Hartmann number, $B_o L\sqrt{\sigma_e/\mu_r}$	μ^*	dimensionless viscosity
$\mathbf{J}$	electric current	μ_r	viscosity at reference state
k	thermal conductivity . . . . . W/m K	ω	vorticity
k^*	dimensionless thermal conductivity	ψ	stream function
k_r	thermal conductivity at reference state	Ψ	dimensionless stream function
L	length of the enclosure . . . . . m	ρ	density . . . . . kg/m^3
Nu	local Nusselt number	σ_e	electrical conductivity of the medium
$\overline{Nu}$	average Nusselt number	τ	dimensionless time
Pr	Prandtl number, $\mu_r/(\rho_r\alpha_r)$	θ	temperature . . . . . °C
p	pressure . . . . . Pa	θ_m	density inversion parameter
Ra	Rayleigh number, $\frac{\mathbf{g}\beta(\theta_h-\theta_c)^b L^3}{\mu_r\rho_r\alpha_r}$	Ω	dimensionless vorticity
T	dimensionless temperature		
T_m	dimensionless density inversion parameter, $\frac{\theta_m-\theta_r}{\theta_h-\theta_c}$	*Subscripts*	
t	time . . . . . s	c	cold wall
u, v	velocity components . . . . . m/s	h	hot wall
U, V	dimensionless velocity components	r	reference state

ied by Zhong et al. [16]. The effect of temperature dependent fluid properties on natural convection in a cavity is investigated by Emery and Lee [17]. They found that though the changes were made in flow and temperature fields there was essentially no change in average Nusselt number. The effect of temperature dependent fluid properties of buoyancy driven convection of air in a horizontal annulus is investigated by Shahraki [18]. He found that the variable viscosity had a strongest effect on fluid velocity while the effects of variable thermal conductivity were in temperature field and local Nusselt numbers.

Rudraiah et al. [6,7] investigated numerically the effect of magnetic field on natural convection in a rectangular enclosure. They found that the magnetic field decreases the rate of heat transfer. The influence of a uniform external magnetic field on natural convection in a square cavity is studied numerically by Krakov and Nikiforov [8]. Buoyancy induced convection in a rectangular cavity with a horizontal temperature gradient in a strong, uniform magnetic field is investigated by Aleksandrova and Molokov [9]. They found that the flow pattern differs significantly for considering the magnetic field orientations. Kenjeres and Hanjalic [19] studied the effects of orientation and distribution of an external magnetic field on heat transfer in thermal convection of electrically conducting fluids. Hossain et al. [20] numerically investigated buoyancy and thermocapillary driven convection of an electrically conducting fluid in an enclosure with internal heat generation. They found that increase in the value of heat generation causes the development of more cells inside the cavity.

A numerical study on unsteady two-dimensional natural convection of an electrically conducting fluid in a laterally and volumetrically heated square cavity under the influence of a magnetic field is investigated by Sarris et al. [21]. They concluded that the heat transfer is enhanced with increasing internal heat generation parameter, but no significant effect of the magnetic field is observed due to the small range of the Hartmann numbers. Chenoweth and Paolucci [22] studied natural convection of air in an enclosure with large horizontal temperature difference. Vierendeels et al. [23] made a benchmark solution for problem of natural convection in an enclosure with large temperature difference. The aim of this paper is to study the effect of temperature dependent fluid properties on MHD convection of water near its density maximum in the differentially heated enclosure.

2. Mathematical formulation

Consider a two-dimensional cavity of width L and height H filled with pure water as shown in Fig. 1. The vertical isothermal side walls of the cavity are maintained at different temperatures θ_h and θ_c, with $\theta_h > \theta_c$ while the horizontal walls of the cavity are adiabatic. The gravity acts in the downwards direction. The velocity components u and v are taken in the x and y directions respectively. It is also assumed that the uniform magnetic field $\mathbf{B} = B_x\mathbf{e}_x + B_y\mathbf{e}_y$ of constant magnitude $B_o = \sqrt{(B_x^2 + B_y^2)}$ is applied, where $\mathbf{e}_x$ and $\mathbf{e}_y$ are unit vectors in Cartesian coordinate system. The orientation of the magnetic field form an angle ϕ with horizontal axis such that $\tan\phi = B_y/B_x$. The electric current $\mathbf{J}$ and the electromagnetic force $\mathbf{F}$ are defined by $\mathbf{J} = \sigma_e(\mathbf{V}\times\mathbf{B})$ and $\mathbf{F} = \sigma_e(\mathbf{V}\times\mathbf{B})\times\mathbf{B}$ respectively. The following assumptions are taken for this study. The density, thermal conductivity and viscosity of the water are varying with temperature and other properties are constant. The

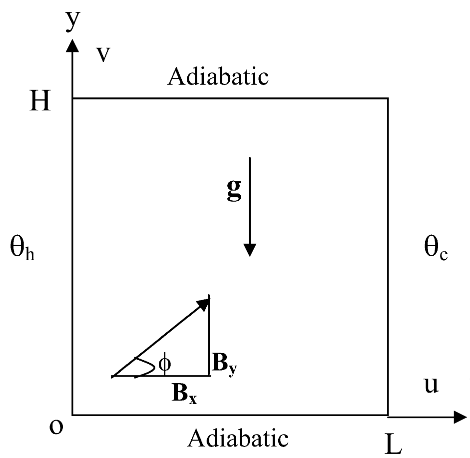

Fig. 1. Physical configuration.

flow is two-dimensional, laminar and incompressible. The radiation, viscous dissipation, induced electric current and Joule heating are neglected. The density of the water varies non-linearly as [2] $\rho = \rho_m[1-\beta|\theta-\theta_m|^b]$, where ρ_m $(=999.972)$ is the maximum density of water, $\beta = 9.297173\times 10^{-6}$, and $b = 1.894816$. The viscosity of the water is assumed to vary with temperature as

$$\mu(\theta) = a + b\theta + c\theta^2 + d\theta^3 \tag{1}$$

where a $(=1.791084)$, b $(=-6.144\times 10^{-2})$, c $(=1.451\times 10^{-3})$ and d $(=-1.6826\times 10^{-5})$ are the temperature coefficient of the viscosity of the water. The equation may be rewritten as

$$\frac{\mu}{\mu_r} = 1 + A_1\epsilon T + A_2\big[(1+\epsilon T)^2 - 1\big] + A_3\big[(1+\epsilon T)^3 - 1\big] \tag{2}$$

where $\epsilon = \frac{\theta_h-\theta_c}{\theta_r}$, $A_1 = \frac{b\theta_r}{\mu_r}$, $A_2 = \frac{c{\theta_r}^2}{\mu_r}$, $A_3 = \frac{d{\theta_r}^3}{\mu_r}$. ϵ $(\leqslant 0.6)$ is known as reference temperature parameter [22]. The thermal conductivity of the water is assumed to vary with temperature as

$$k(\theta) = a_1 + b_1\theta + c_1\theta^2 + d_1\theta^3 \tag{3}$$

where a_1 $(=0.561965)$, b_1 $(=2.15346\times 10^{-3})$, c_1 $(=-1.55141\times 10^{-5})$ and d_1 $(=1.01689\times 10^{-7})$ are the temperature coefficient of the thermal conductivity of the water. The equation may be rewritten as

$$\frac{k}{k_r} = 1 + B_1\epsilon T + B_2\big[(1+\epsilon T)^2 - 1\big] + B_3\big[(1+\epsilon T)^3 - 1\big] \tag{4}$$

where $B_1 = \frac{b_1\theta_r}{k_r}$, $B_2 = \frac{c_1{\theta_r}^2}{k_r}$, $B_3 = \frac{d_1{\theta_r}^3}{k_r}$.

The governing equations for viscous incompressible electrically conducting fluid with temperature dependent fluid properties are

$$\frac{\partial u}{\partial x} + \frac{\partial v}{\partial y} = 0 \tag{5}$$

$$\rho_r\left(\frac{\partial u}{\partial t} + u\frac{\partial u}{\partial x} + v\frac{\partial u}{\partial y}\right) + \frac{\partial P}{\partial x} = \frac{\partial}{\partial x}\left(2\mu\frac{\partial u}{\partial x}\right) + \frac{\partial}{\partial y}\left(\mu\frac{\partial u}{\partial y} + \mu\frac{\partial v}{\partial x}\right) + \sigma_e B_0^2(v\sin\phi\cos\phi - u\sin^2\phi) \tag{6}$$

$$\rho_r\left(\frac{\partial v}{\partial t} + u\frac{\partial v}{\partial x} + v\frac{\partial v}{\partial y}\right) + \frac{\partial P}{\partial y} = \frac{\partial}{\partial x}\left(\mu\frac{\partial u}{\partial y} + \mu\frac{\partial v}{\partial x}\right) + \frac{\partial}{\partial y}\left(2\mu\frac{\partial v}{\partial y}\right) - \rho g + \sigma_e B_0^2(u\sin\phi\cos\phi - v\cos^2\phi) \tag{7}$$

From Eqs. (6) and (7), the vorticity equation takes the form

$$\begin{aligned}\rho_r&\left\{\frac{\partial\omega}{\partial t} + u\frac{\partial\omega}{\partial x} + v\frac{\partial\omega}{\partial y}\right\} \\ &= \mu\left(\frac{\partial^2\omega}{\partial x^2} + \frac{\partial^2\omega}{\partial y^2}\right) + 2\frac{\partial\mu}{\partial x}\frac{\partial\omega}{\partial x} + 2\frac{\partial\mu}{\partial y}\frac{\partial\omega}{\partial y} + 4\frac{\partial^2\mu}{\partial x\partial y}\frac{\partial v}{\partial y} \\ &\quad + \left[\frac{\partial^2\mu}{\partial x^2} - \frac{\partial^2\mu}{\partial y^2}\right]\left(\frac{\partial u}{\partial y} + \frac{\partial v}{\partial x}\right) + \rho_m g\beta\frac{\partial|\theta-\theta_m|^b}{\partial x} \\ &\quad + \sigma_e B_0^2\left[\sin\phi\cos\phi\left(\frac{\partial u}{\partial x} - \frac{\partial v}{\partial y}\right) + \left(\sin^2\phi\frac{\partial u}{\partial y} - \cos^2\phi\frac{\partial v}{\partial x}\right)\right]\end{aligned} \tag{8}$$

The energy equation is as follows

$$\frac{\partial\theta}{\partial t} + u\frac{\partial\theta}{\partial x} + v\frac{\partial\theta}{\partial y} = \frac{\partial}{\partial x}\left(\frac{k}{\rho_r c_p}\frac{\partial\theta}{\partial x}\right) + \frac{\partial}{\partial y}\left(\frac{k}{\rho_r c_p}\frac{\partial\theta}{\partial y}\right) \tag{9}$$

where θ is the temperature of the fluid, ρ_r is the density, p is the pressure, μ is the viscosity, k is the thermal conductivity, g is the gravity, p is the pressure, c_p is the specific heat and t is the time.

The initial and boundary conditions are

$$t=0:\quad u=v=0,\quad \theta=\theta_c,\quad 0\leqslant x\leqslant L,\ 0\leqslant y\leqslant H$$
$$t>0:\quad u=v=0,\quad \frac{\partial\theta}{\partial y}=0,\quad y=0\,\&\,H$$
$$u=v=0,\quad \theta=\theta_h,\quad x=0$$
$$u=v=0,\quad \theta=\theta_c,\quad x=L$$

The following non-dimensional variables are used

$$(X,Y)=\frac{(x,y)}{L},\qquad (U,V)=\frac{(u,v)}{\mu_r/L\rho_r},\qquad \tau=\frac{t}{L^2\rho/\mu_r}$$
$$\mu^*=\frac{\mu}{\mu_r},\qquad k^*=\frac{k}{k_r},\qquad \Psi=\frac{\psi}{\mu_r/\rho_r}$$
$$\Omega=\frac{\omega}{\mu_r/\rho_r L^2},\qquad T=\frac{\theta-\theta_r}{\theta_h-\theta_c}$$

After nondimensionalization, the governing equations are

$$\begin{aligned}&\frac{\partial\Omega}{\partial\tau} + U\frac{\partial\Omega}{\partial X} + V\frac{\partial\Omega}{\partial Y} \\ &= \mu^*\nabla^2\Omega + \frac{Ra}{Pr}\frac{\partial|T-T_m|^b}{\partial X} + 2\frac{\partial\mu^*}{\partial X}\frac{\partial\Omega}{\partial X} \\ &\quad + 2\frac{\partial\mu^*}{\partial Y}\frac{\partial\Omega}{\partial Y} + 4\frac{\partial^2\mu^*}{\partial X\partial Y}\frac{\partial V}{\partial Y} + \left[\frac{\partial^2\mu^*}{\partial X^2} - \frac{\partial^2\mu^*}{\partial Y^2}\right] \\ &\quad \times\left(\frac{\partial U}{\partial Y} + \frac{\partial V}{\partial X}\right) + Ha^2\left[\sin\phi\cos\phi\left(\frac{\partial U}{\partial X} - \frac{\partial V}{\partial Y}\right)\right.\end{aligned}$$

$$+\left(\sin^2\phi\frac{\partial U}{\partial Y}-\cos^2\phi\frac{\partial V}{\partial X}\right)\Bigg] \tag{10}$$

$$\nabla^2\Psi=-\Omega \tag{11}$$

$$\frac{\partial T}{\partial\tau}+U\frac{\partial T}{\partial X}+V\frac{\partial T}{\partial Y}=\frac{1}{Pr}\left[\frac{\partial}{\partial X}\left(k^*\frac{\partial T}{\partial x}\right)+\frac{\partial}{\partial Y}\left(k^*\frac{\partial T}{\partial Y}\right)\right] \tag{12}$$

$$U=\frac{\partial\Psi}{\partial Y}\quad\text{and}\quad V=-\frac{\partial\Psi}{\partial X} \tag{13}$$

The initial and boundary conditions in the dimensionless form are

$$t=0:\quad U=V=\Psi=0,\quad \Omega=T=0\quad 0\leqslant X\leqslant 1,\ 0\leqslant Y\leqslant 1$$

$$t>0:\quad U=V=\Psi=0,\quad \frac{\partial T}{\partial Y}=0,\quad \Omega=-\frac{\partial^2\Psi}{\partial X^2}\quad X=0\,\&\,1$$

$$U=V=\Psi=0,\quad T=1,\quad \Omega=-\frac{\partial^2\Psi}{\partial Y^2},\quad Y=0$$

$$U=V=\Psi=0,\quad T=0,\quad \Omega=-\frac{\partial^2\Psi}{\partial Y^2},\quad Y=1$$

The non-dimensional parameters that appear in the equations are $Ha=B_oL\sqrt{\sigma_e/\mu_r}$, Hartmann number, $T_m=\frac{(\theta_m-\theta_r)}{(\theta_h-\theta_c)}$, density inversion parameter, $Ra=\frac{g\beta(\theta_h-\theta_c)^bL^3}{\mu_r\alpha_r/\rho_r}$, the Rayleigh number, $Pr=\frac{\mu_r}{\rho_r\alpha_r}$, the Prandtl number. The local Nusselt number which accounts for the rate of heat transfer across the enclosure is computed at hot wall and defined by $Nu=-k^*\frac{\partial T}{\partial Y}|_{X=0}$, and the average Nusselt number is given by $\overline{Nu}=\int_0^1 Nu\,\mathrm{d}Y$.

3. Numerical method

The non-dimensional equations subject to the boundary conditions are solved by control volume method. The QUICK scheme is used for the convection terms and central difference scheme is used for diffusion terms. The solution domain consists a number of grid points at which discretization equations are applied. The uniform grid has been selected in both X and Y directions. The grid size were tested from 21×21 to 121×121 for $Ra=10^6$, $Pr=11.6$ and constant fluid properties, i.e., ($T_m=0.0$ and $\epsilon=0.0$). It is observed from the grid independence test that a 81×81 uniform grid is enough to investigate the problem. The time step is chosen to be uniform $\Delta\tau=10^{-4}$. The resulting algebraic equations for energy and vorticity are solved by iterative method whereas Successive Over Relaxation (SOR) method is used to solve the equation for stream function. The relaxation parameter is taken to be 1.5. Thus, having calculated the temperature and vorticity values at an advance point in time $\tau=(n+1)\,\mathrm{d}\tau$, using their respective solution given at $\tau=(n)\,\mathrm{d}\tau$ ($n=0$ corresponds to the initial condition), the stream function is solved for its solution at this advanced time step. The resulting stream function values are then used to determine the velocity components and the boundary values of the vorticity from the relation $\Omega=\frac{\Psi_{i,2}-8\Psi_{i,1}}{2h^2}$. Thus, the sequence beginning with the solution of the energy equation is applied repeated until the desired accuracy of results are obtained. The convergence criterion used for the field variables ϕ ($=T,\Omega,\ \Psi$) is $|\frac{\phi_{(n+1)}(i,j)-\phi_{(n)}(i,j)}{\phi_{(n+1)}(i,j)}|\leqslant 10^{-6}$. The validation of present computational code is verified against the existing results for natural convection in a square cavity filled with either air [17,24] or water near its density maximum [1,13] and magnetic force [6] and are shown in Tables 1–3. A in-house computer code is developed and computations are performed on Intel Xeon 3.6 GHz with 2.0 GB RAM workstations.

Table 1
Comparison of $\overline{Nu}$ results with previous works for square cavity with constant fluid properties

Pr	Ra	$\overline{Nu}$		
		Davis [24]	Emery & Lee [17]	Present
0.1	10^4	–	2.011	2.126
	10^5	–	3.794	3.972
0.71	10^3	1.116	–	1.110
	10^4	2.234	–	2.235
	10^5	4.510	–	4.496
	10^6	8.869	–	8.658
1.0	10^4	–	2.226	2.247
	10^5	–	4.500	4.572

Table 2
Comparison of $\overline{Nu}$ results for different density inversion parameters with previous works for square cavity with constant fluid properties except density

Ra	T_m	$\overline{Nu}$		
		Nansteel et al. [1]	Tong [13]	Present
10^3	0.5	1.0009	1.0007	0.9914
	1.0	1.1190	1.1860	1.1122
10^4	0.5	1.076	1.0655	1.0689
	1.0	2.278	2.2739	2.2443

Table 3
Comparison of $\overline{Nu}$ results with previous works for effect of magnetic force on natural convection in a square cavity and $Gr=2\times 10^5$

Ha	$\overline{Nu}$	
	Rudraiah et al. [6]	Present
0	4.9198	5.0025
10	4.2053	4.8148
50	2.8442	2.8331
100	1.4317	1.4341

4. Results and discussion

Magnetohydrodynamic convection of cold water near its density maximum with temperature dependent fluid properties is investigated numerically by reference temperature method. The Prandtl number $Pr=11.6$ and reference temperature $\theta_r=3.98$ are taken for all cases. The results are discussed for variable viscosity, variable thermal conductivity and both variable viscosity and thermal conductivity of water for different density inversion parameter T_m, Rayleigh numbers Ra, reference temperature parameter ϵ and Hartman number Ha.

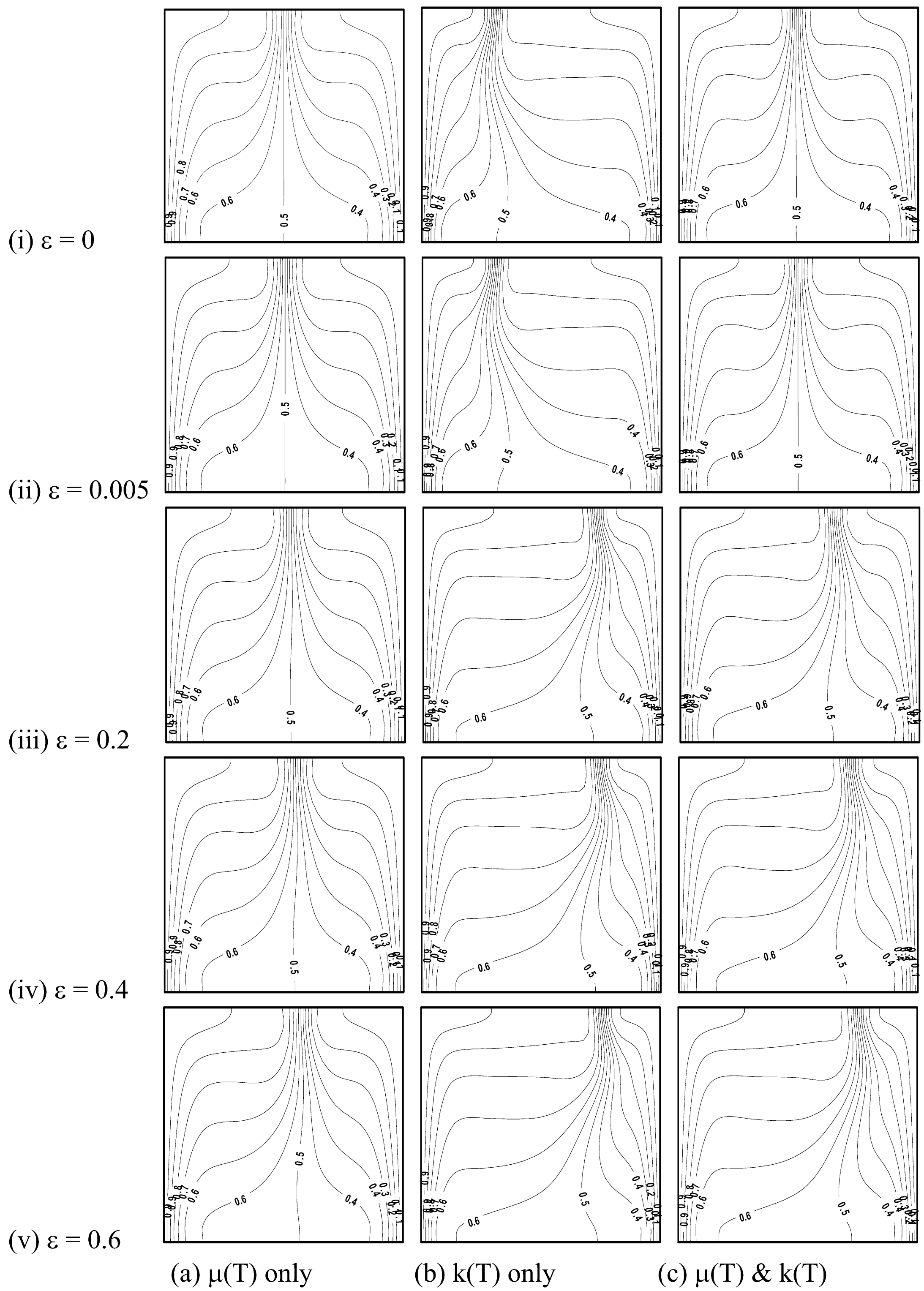

Fig. 2. Isotherms for different ε, $T_m = 0.5$, $Ha = 25$, $\phi = 0°$ and $Ra = 10^6$.

Fig. 2 shows the isotherms for variable viscosity, variable thermal conductivity and both variable viscosity and thermal conductivity of water for different reference temperature parameter ϵ, $Ra = 10^6$, $T_m = 0.5$, $Ha = 25$ and $\phi = 0°$. The density maximum plane is at middle of the cavity for variable viscosity and variable thermal conductivity cases when $\epsilon = 0$, that is, the density gradient is approximately symmetric with respect to the vertical mid plane. The density maximum plane is between hot wall and center of the cavity for both variable viscosity and thermal conductivity case. There is a temperature stratification in the vertical direction and a feeble thermal boundary layer is established along the side walls. Increasing $\epsilon = 0.2$ there is no

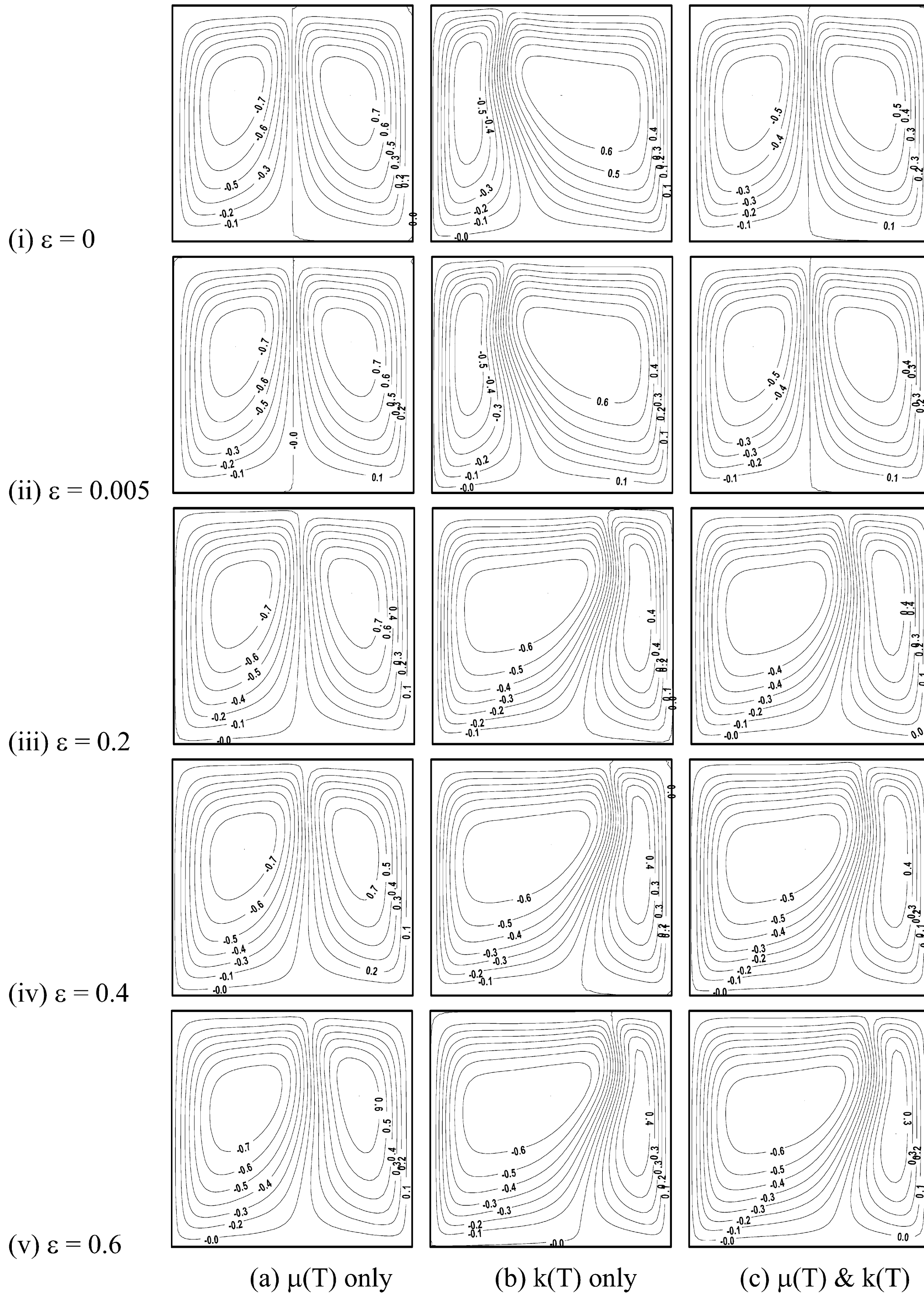

Fig. 3. Streamlines for different ε, $T_m = 0.5$, $Ha = 25$, $\phi = 0°$ and $Ra = 10^6$.

change in temperature dependent viscosity case. The density maximum plane moves from center of the cavity towards cold wall for variable thermal conductivity case. The temperature field is very much affect in the case of both variable viscosity and thermal conductivity. The density maximum plane moves from hot wall side to cold wall side. Further increasing ϵ the same behaviour is observed for all temperature dependent fluid properties.

The corresponding streamlines are depicted in Fig. 3. For all values of ϵ there exists dual cell structure. The flow consists of a symmetric counter rotating cell pattern with up flow of warm and cold fluid near the vertical hot and cold walls and down flow near the vertical mid plane (density maximum region) of the cavity. But the dual cell structure is depending on the values of ϵ and temperature dependent fluid properties. When $\epsilon = 0$ the two cells are in same size for variable viscosity and both

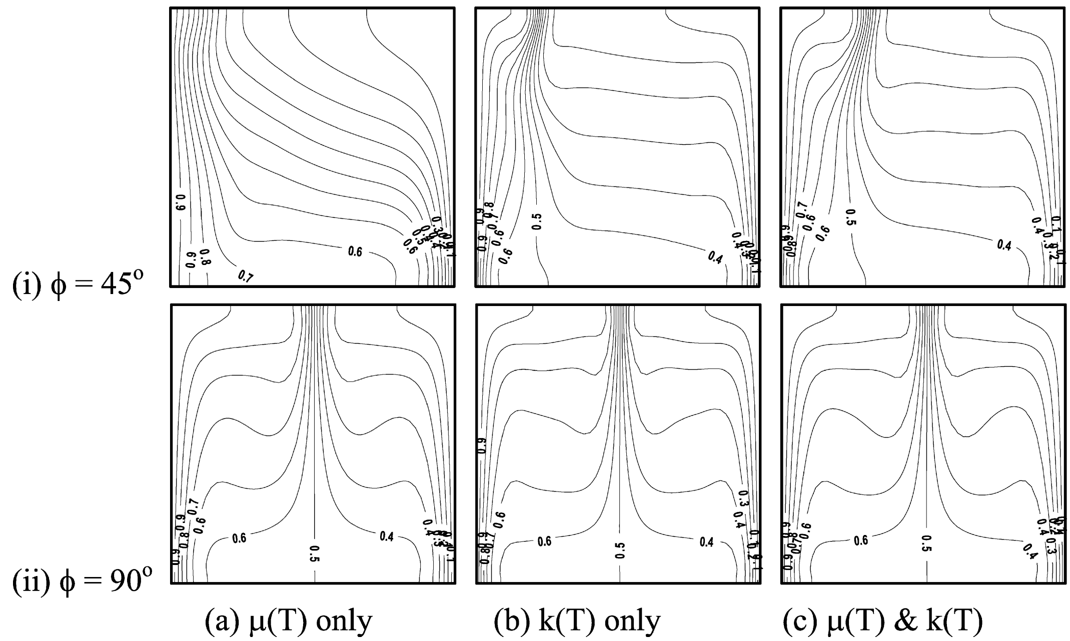

Fig. 4. Isotherms for different ϕ, $T_m = 0.5$, $Ha = 25$, $\varepsilon = 0.2$ and $Ra = 10^6$.

variable viscosity and variable thermal conductivity cases. But the circulation rate of the cell is high in the case of variable viscosity than the case both variable viscosity and variable thermal conductivity. For temperature dependent thermal conductivity, the cold cell is strengthened and hot cell is weakened. Increasing $\epsilon = 0.2$ there is no change in variable viscosity case. For the case of variable thermal conductivity the size of the hot cell is increased and cold cell is suppressed. For both variable viscosity and thermal conductivity case flow pattern is also changed significantly. The size of the hot cell grows and suppresses its counter part. Further increasing ϵ there is no change for variable viscosity and variable thermal conductivity cases. But both fluid properties varying case, the clockwise rotation cell is increased in its size and strengthens when increasing the reference temperature parameter. Two convective cells are separated by the $\Psi = 0$ plane at all times. It is clearly seen from the figures that the flow field is affected by variable fluid properties.

The effect of direction of external magnetic field on temperature distribution is depicted in Fig. 4. When $\phi = 45°$ the density maximum plane coincides with the hot wall for variable viscosity case and near to the hot wall for other cases. The temperature stratification diminishes for temperature dependent viscosity case. The density maximum plane is at middle of the cavity for all cases of temperature dependent fluid properties when $\phi = 90°$. The thermal boundary layer is formed near both heated and cooled walls. Thus thin layers formed which are associated with high rates of heat transfer. But $\phi = 0°$ the density maximum plane is at middle of the cavity for variable viscosity and variable thermal conductivity cases and near to the cold wall for both variable viscosity and thermal conductivity case. Comparing these figures the temperature distribution is affected very much when $\phi = 45°$. This is due to the retarding effect of Lorentz force.

The streamlines for different direction of external magnetic field is displayed in Fig. 5. The dual cell structure is affected much when the direction of magnetic field is inclined than vertical or horizontal. The clockwise cell shrinks in its size and counter clockwise cell grows in its size, strengthen and occupies the majority of the cavity for variable viscosity case. It can be seen from the figure that as the direction of external magnetic field changes from horizontal to inclined the flow rate of cells decreases. For vertical magnetic field the flow has high circulation rate and provide high heat transfer rate. For $\phi = 90°$ the flow field is strengthened for the temperature dependent viscosity case while the flow field is weakened for considering both fluid properties. Fig. 6 shows the isotherms and streamlines for $\phi = 0°$, $T_m = 0.5$, $Ha = 100$, $\epsilon = 0.2$ and $Ra = 10^6$. The isotherms become almost vertical lines, resembling the conduction type heat transfer due to high magnetic field strength. The core region of streamlines is elongated in vertical direction. There is no change in flow filed when changing the temperature dependent fluid properties for high values of Hartmann number.

Fig. 7 shows the average Nusselt number for different values of direction of external magnetic field, ϕ. It is seen from Fig. 7 that the heat transfer rate is minimum when $\phi = 0°$, that is horizontal magnetic field. Heat transfer is enhanced when the angle of external magnetic field is $\phi = 90°$. It is also observed from the figure that the heat transfer rate is high for the temperature dependent viscosity case. Fig. 8 shows the effect of density inversion parameter on average Nusselt number with $\phi = 0°$, $\epsilon = 0.2$ and $Ra = 10^6$. When increasing the Hartmann number the heat transfer rate is decreased. It is also found that the average Nusselt number gets minimum in the density maximum region, that is $T_m = 0.5$. For such a situation, the dual cell structure inhibits the direct convective transfer of energy from the hot to the cold cell. This phenomenon results essentially from the inversion of the fluid density at 4 °C and is one of its most

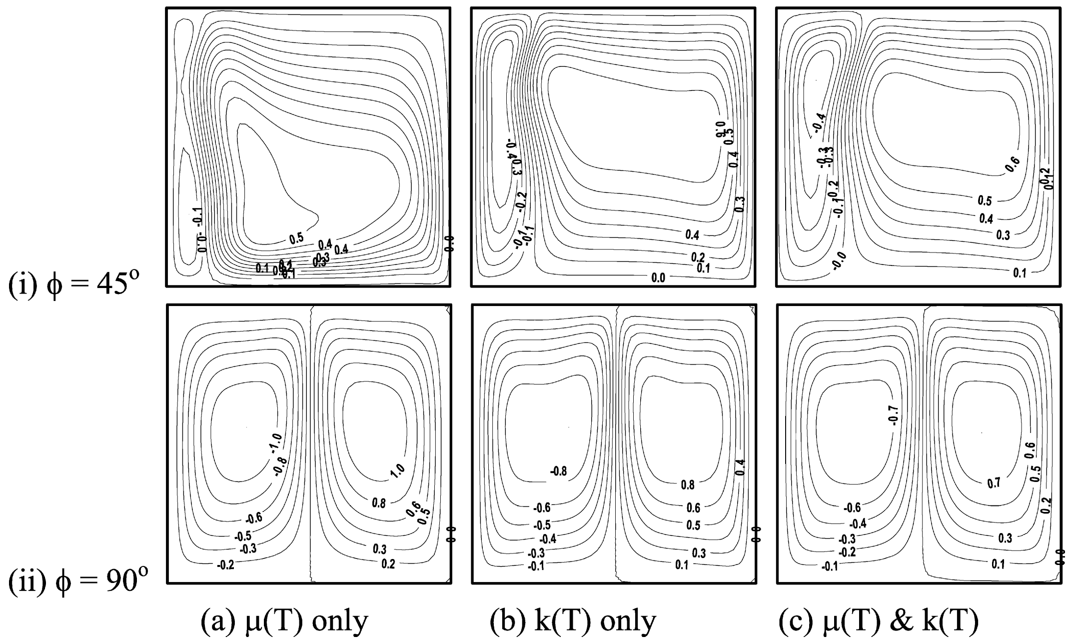

Fig. 5. Streamlines for different ϕ, $T_m = 0.5$, $Ha = 25$, $\varepsilon = 0.2$ and $Ra = 10^6$.

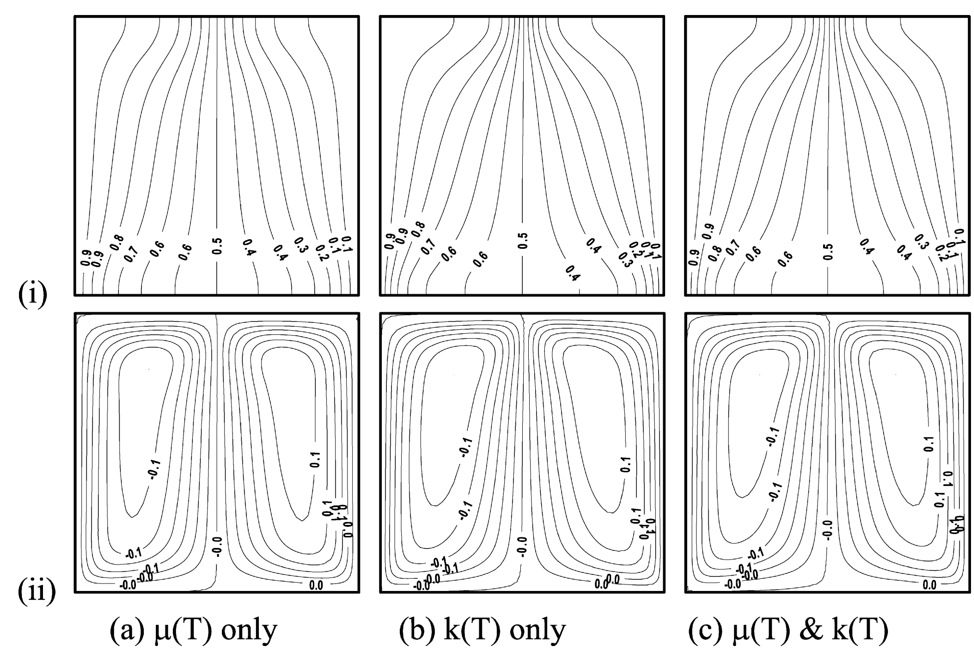

Fig. 6. Isotherms and streamlines for $\phi = 0°$, $T_m = 0.5$, $Ha = 100$, $\varepsilon = 0.2$ and $Ra = 10^6$.

significant effects on the mechanism of heat transfer by convection of water within a cavity. So heat transfer rate is reduced in such a situation for all values of Rayleigh numbers. For sufficiently large Hartmann number in density maximum region the convection is completely suppressed as all temperature dependent fluid properties. In such situation the heat transfer is dominated by conduction.

The average Nusselt number for different reference temperature parameters with $T_m = 0.5$, $Ha = 25$ and $\phi = 0°$ is displayed in Fig. 9. It is found that increasing the Raleigh number increases the heat transfer rate for all values of ϵ. Also observed that there is no significant effect on average Nusselt number when changing the reference temperature parameter ϵ. But it is evidently seen from the figure that changing the temperature-dependent properties produces the significant effect on average heat transfer rate. The average heat transfer rate considering temperature-dependent viscosity are higher than considering temperature-dependent thermal conductivity and both temperature-dependent viscosity and thermal conductivity for all values of Ra. Fig. 10 shows the average Nusselt number for different Hartmann number. Increasing Hartmann number decreased the heat transfer rate. In order to find the effect of direction of external magnetic field on heat transfer rate, average Nusselt number is plotted as a function of ϕ and shown

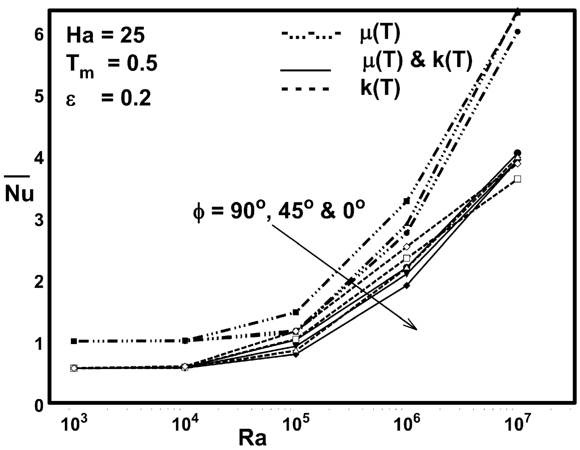

Fig. 7. Average Nusselt number for different ϕ, $T_m = 0.5$, $Ha = 25$, $\varepsilon = 0.2$.

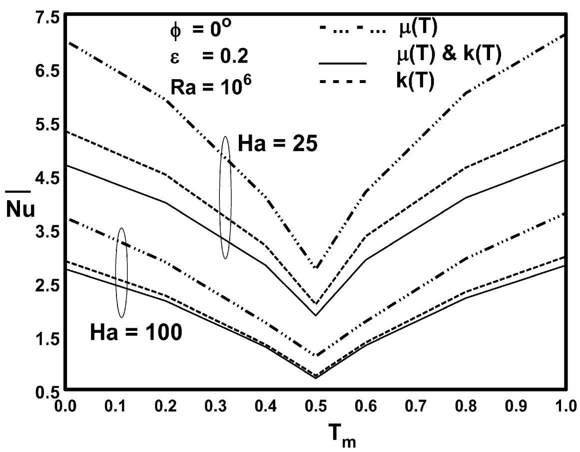

Fig. 8. Average Nusselt number vs $T_m = 0.5$ for $\phi = 0°$, $\varepsilon = 0.2$ and $Ra = 10^6$.

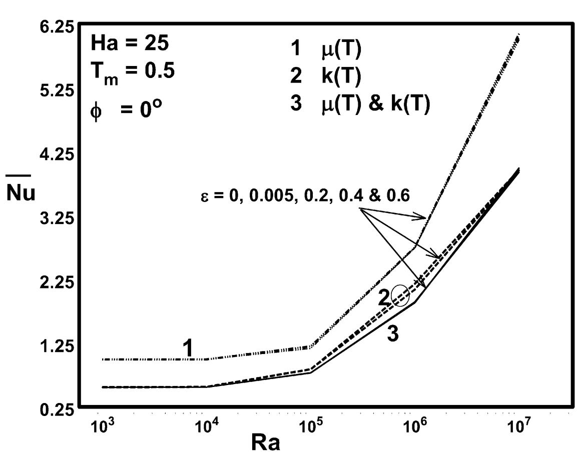

Fig. 9. Average Nusselt number for different ε, $Ha = 25$ and $\phi = 0°$.

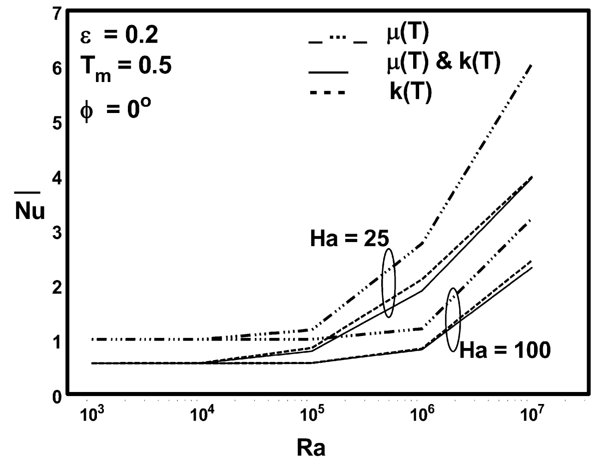

Fig. 10. Average Nusselt number for different Ha, $\varepsilon = 0.2$, $T_m = 0.5$ and $\phi = 0°$.

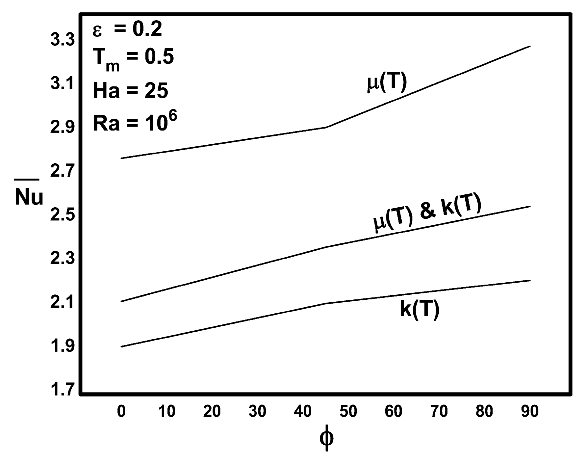

Fig. 11. Average Nusselt number vs ϕ for $\varepsilon = 0.2$, $T_m = 0.5$, $Ha = 25$ and $Ra = 10^6$.

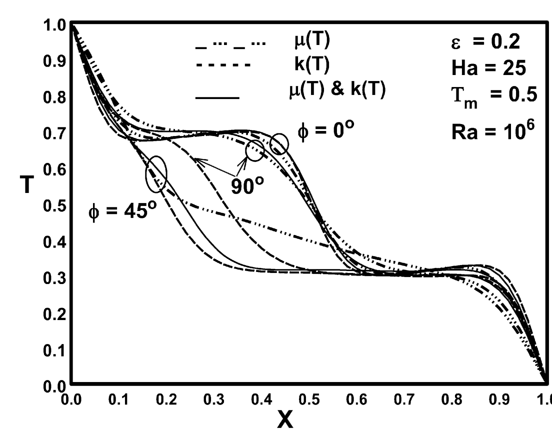

Fig. 12. Temperature along hot wall for different ϕ, $\varepsilon = 0.2$, $T_m = 0.5$, $Ha = 25$ and $Ra = 10^6$.

in Fig. 11. When $\phi = 90°$ provides better heat transfer rate that other two angles of external magnetic field. Heat transfer rate is enhanced when considering temperature-dependent viscosity.

Fig. 12 shows the non-dimensional temperature profiles at middle of the cavity for different values of ϕ, $T_m = 0.5$, $Ha = 25$ and $\epsilon = 0.2$. There is no sharp thermal boundary later formed for all cases. Mid-height velocity profiles for different ϕ, $T_m = 0.5$, $Ha = 25$, $\epsilon = 0.2$ and $Ra = 10^6$ are displayed in Fig. 13. The bidirectional velocity curves clearly show the dual cell structure. The fluid particles are having higher velocity for vertical magnetic field for all cases of temperature dependent fluid properties. This results in the higher heat transfer rate.

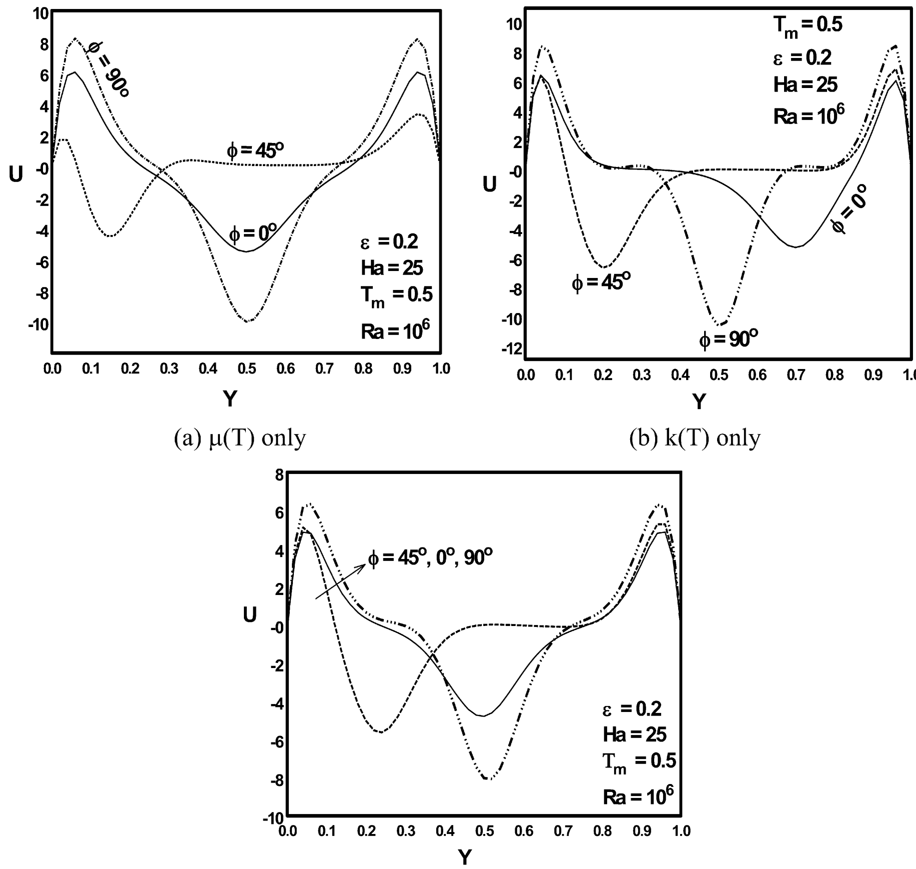

(a) μ(T) only

(b) k(T) only

(c) Both μ(T) and k(T)

Fig. 13. Mid-height velocity profiles for different ϕ with $\varepsilon = 0.2$, $T_m = 0.5$, $Ha = 25$ and $Ra = 10^6$.

5. Conclusion

The effects of temperature dependent properties of water near its density maximum in the presence of uniform magnetic field on fluid flow and heat transfer have been studied for different combination of parameters. Though fluid flow and temperature distributions make a sensitive difference on changing the values of temperature difference parameters, there is no change in average heat transfer rate. The average heat transfer rate considering temperature-dependent viscosity are higher than considering temperature-dependent thermal conductivity and both temperature-dependent viscosity and thermal conductivity for all values of Ra, T_m. The heat transfer rate decreases with an increase of Hartmann number. The velocity and temperature profiles were distorted when the effects of temperature-dependent properties were considered. It is observed that the density inversion leaves strong effects on fluid flow and heat transfer due to the formation of bi-cellular structure. The formation of dual cell structure and strength of each cell is always depends on the density inversion parameter and Rayleigh number. The heat transfer rate behaves non-linearly with density inversion parameter. The heat transfer rates are found to increase with increasing Rayleigh number.

Acknowledgements

The funding for the post-doctorate research fellowship for S. Sivasankaran from National Science Council of ROC in Taiwan through Project No. NSC95-2811-E006-025 is greatly appreciated.

References

[1] M.W. Nansteel, K. Medjani, D.S. Lin, Natural convection of water near its density maximum in a rectangular enclosure: Low Rayleigh number calculations, Phys. Fluids 30 (2) (1987) 312–317.

[2] C.J. Ho, F.J. Tu, Numerical study on oscillatory convection of cold water in a tall vertical enclosure, Int. J. Numer. Methods Heat Fluid Flow 9 (1999) 487–508.

[3] C.J. Ho, F.J. Tu, Visualization and prediction of natural convection of water near its density maximum in a tall rectangular enclosure at high Rayleigh numbers, J. Heat Transfer 123 (2001) 84–95.

[4] C.J. Ho, F.J. Tu, Transition to oscillatory natural convection of water near its density maximum in a tall enclosure, Int. J. Numer. Methods Heat Fluid Flow 11 (7) (2001) 626–641.

[5] P. Kandaswamy, S. Sivasankaran, N. Nithyadevi, Transient natural convection of water in a square cavity with partially active vertical walls, Int. J. Heat Mass Transfer 50 (2007) 942–948.

[6] N. Rudraiah, R.M. Barron, M. Venkatachalappa, C.K. Subbaraya, Effect of a magnetic field on free convection in a rectangular enclosure, Int. J. Engrg. Sci. 33 (8) (1995) 1075–1084.

[7] N. Rudraiah, M. Venkatachalappa, C.K. Subbaraya, Combined surface tension and buoyancy driven convection in a rectangular open cavity in

the presence of a magnetic field, Int. J. Non-Linear Mech. 30 (5) (1995) 759–770.

[8] M.S. Krakov, I.V. Nikiforov, To the influence of uniform magnetic field on thermomagnetic convection in square cavity, J. Magn. Magn. Mater. 252 (2002) 209–211.

[9] S. Aleksandrova, S. Molokov, Three-dimensional buoyant convection in a rectangular cavity with differentially heated walls in a strong magnetic field, Fluid Dynam. Res. 35 (2004) 37–66.

[10] J. Hallett, The temperature dependence of the viscosity of supercooled water, Proc. Phys. Soc. 82 (1963) 1046–1050.

[11] M.D. Souza, R.F.D. Miranda, H.A. Machado, Natural convection in enclosures with variable fluid properties, Int. J. Numer. Methods Heat Fluid Flow 13 (8) (2003) 1079–1096.

[12] S. Sivasankaran, P. Kandaswamy, Double diffusive convection of water in a rectangular partitioned enclosure with temperature dependent species diffusivity, Int. J. Fluid Mech. Res. 33 (4) (2006) 345–361.

[13] W. Tong, Aspect ratio effect on natural convection in water near its density maximum temperature, Int. J. Heat Fluid Flow 20 (1999) 624–633.

[14] M. Ishikawa, T. Hirata, S. Noda, Numerical simulation of natural convection with density inversion in a square cavity, Numer. Heat Transfer Part A 37 (2000) 395–406.

[15] H.S. Mahdi, K.R. Wedgworth, Natural convention in a square cavity with temperature dependent viscosity, Proc. ASME Heat Transfer Div. 317 (1) (1995) 81–95.

[16] Z.Y. Zhong, K.T. Yang, J.R. Lloyd, Variable property effects in laminar natural convection in a square enclosure, J. Heat Transfer 107 (1985) 133–138.

[17] A.F. Emery, J.W. Lee, The effects of property variations on natural convection in a square enclosure, J. Heat Transfer 121 (1999) 57–62.

[18] F. Shahraki, Modeling of buoyancy-driven flow and heat transfer for air in an horizontal annulus: Effects of vertical eccentricity and temperature-dependent properties, Numer. Heat Transfer Part A 42 (2002) 603–621.

[19] S. Kenjeres, K. Hanjalic, Numerical simulation of magnetic control of heat transfer in thermal convection, Int. J. Heat Fluid Flow 25 (2004) 559–568.

[20] M.A. Hossain, M.Z. Hafiz, D.A.S. Rees, Buoyancy and thermocapillary driven convection flow of an electrically conducting fluid in an enclosure with heat generation, Int. J. Thermal Sci. 44 (2005) 676–684.

[21] I.E. Sarris, S.C. Kakarantzas, A.P. Grecos, N.S. Vlachos, MHD natural convection in a laterally and volumetrically heated square cavity, Int. J. Heat Mass Transfer 48 (2005) 3443–3453.

[22] D.R. Chenoweth, S. Paolucci, Natural convection in an enclosed vertical air layer with large temperature differences, J. Fluid Mech. 169 (1986) 173–210.

[23] J. Vierendeels, B. Merci, E. Dick, Benchmark solutions for the natural convective heat transfer problem in a square cavity with large horizontal temperature differences, Int. J. Numer. Methods Heat Fluid Flow 13 (8) (2003) 1057–1078.

[24] G.D. Vahl Davis, Natural convection of air in a square cavity a bench mark numerical solutions, Int. J. Numer. Methods Fluids 3 (1983) 249–264.